ELSEVIER

Thermochimica Acta 282/283 (1996) 43–49

thermochimica
acta

The kinetics of thermal dehydration of calcium copper acetate hexahydrate[1]

Yoshio Masuda[a,*], Sugiko Shirotori[b], Kazue Minagawa[c], P.K. Gallagher[d], Zhimin Zhong[d]

[a] *Department of Environmental Science, Faculty of Science, Niigata University, Niigata 950-21, Japan*
[b] *Graduate School of Science and Technology, Niigata University, Niigata 950-21, Japan*
[c] *Department of Chemistry, Faculty of Science, Niigata University, Niigata 950-21, Japan*
[d] *Department of Chemistry and Materials Science and Engineering, The Ohio State University, Columbus, OH 43210-1173, USA*

Abstract

The kinetics of the thermal dehydration of crushed crystals of $CaCu(CH_3CO_2)_4 \cdot 6H_2O$ in a flowing nitrogen atmosphere have been studied by means of isothermal gravimetry.

At higher temperatures than 85°C the dehydration seemed to be described by three-dimensional phase boundary reactions, $R_3(\alpha)$. At temperatures lower than 80°C, the initial part of the dehydration could be described by phase boundary reactions, $R_3(\alpha)$, that of the middle part follows the Avrami–Erofeev type reaction, $A_{2.5}(\alpha)$, and then the kinetics of the final part followed diffusion-controlled models. These transitions of the dehydration mechanisms have been discussed on the basis of the diffusion process of dissociated water molecules.

Keywords: Calcium acetate copper hexahydrate; Isothermal gravimetry; Kinetics; Thermal dehydration

1. Introduction

Calcium copper acetate hexahydrate, $CaCu(CH_3CO_2)_4 \cdot 6H_2O$ is a normal paramagnetic crystal and may easily be grown as large prismatic crystals from solutions of calcium acetate and copper acetate. Because of the interest in the compound's magnetic behavior, its magnetic susceptibility, electron paramagnetic resonance (EPR) spec-

---

* Corresponding author.

[1] Dedicated to Dr. Takeo Ozawa in honor of his 65th birthday.

SSDI 0040-6031(95)02799-6

trum, and its specific heat have been measured [1–4]. The electronic properties of this compound have also attracted some interest, and the electron spin resonance (ESR) spectrum of a single crystal and the compound's electronic spectra have been measured [5, 6]. Smith applied an angular overlap treatment with electrostatic corrections to the *d*-orbital splitting in this hydrate [7].

$CaCu(CH_3CO_2)_4 \cdot 6H_2O$ has also made an interesting contribution to study of the stereochemical diversity of copper compounds. The crystal structure of $CaCu\ (CH_3\ CO_2)_4 \cdot 6H_2O$ is tetragonal with four molecules per unit cell and its space group belongs to I4/m [8, 9]. This compound consists of polymeric chains of bidentate acetate-bridged copper and calcium atoms. The chains aligned along the c-axis, are bound together by "solvent cages" of twelve water molecules. The water molecules only coordinate to calcium ions and their role in the structure is to fill the void of the lattice and to bind the polymeric chains together. Each water molecule is hydrogen-bonded to form clusters of twelve water molecules which have C4h symmetry.

It is interesting to study the behavior of the water molecules held in the crystal structure during thermal dehydration. This paper describes the use of isothermal gravimetry to study the kinetics of the thermal dehydration of crushed calcium copper acetate hexahydrate in a flowing of nitrogen atmosphere.

2. Experimental

A single crystal of calcium copper acetate hexahydrate, $CaCu(CH_3CO_2)_4 \cdot 6H_2O$, was prepared from solutions of calcium acetate and copper acetate. The sample was identified by means of FTIR and dynamic TG. The crystals were crushed with a mortar and pestle and sieved to a narrow fractions of 100–150 mesh sizes.

The isothermal dehydration was followed with a Shinku-Riko TGD-5000 RH differential microbalance equipped with a gold image furnace [10–13]. About 5 mg of sample was weighed into a platinum crucible and set in the microbalance. The furnace was maintained at constant temperatures within ± 0.5 K until the dehydration was complete. The output voltages for the mass loss from the microbalance were amplified and acquired on an Epson PC286 VE microcomputer, via AD converter ICL 7109 modified in 13 bits. For each dehydration process, about 1000 data points relating to the mass loss were collected at given time intervals, and the fraction of dehydration, α was calculated from the data. All measurements were carried out in a flowing nitrogen atmosphere (flow rate 60 $cm^3\ min^{-1}$). The dynamic TG was performed at heating rates of 5–10 K min^{-1} using a Rigaku TAS-200 system.

The X-ray powder diffraction patterns were obtained with a Rigaku Geigerflex Rad-R diffractometer equipped with a standard high-temperature sample holder; CuK_α radiation and a nickel filter were used. The radiation was monochromatized at the counter side using a graphite monochromator. The diffraction data were taken at steps of width 0.02°. Infrared spectra were measured from 400 to 4400 cm^{-1} with a Horiba FTIR 300 spectrophotometer.

3. Results

Fig. 1 shows isothermal thermogravimetric curves, $\alpha(t)$ for the thermal dehydration of $CaCu(CH_3CO_2)_4 \cdot 6H_2O$. It is worth noting that the $\alpha(t)$ curves do not have a sigmoidal character, i.e. the $\alpha(t)$ consists of deceleratory periods only; an acceleratory period is absent from this dehydration. The fact that the dehydrated product phase was amorphous, should also be emphasized.

The kinetics of a solid state reaction are expressed by the equation

$$G(\alpha) = kt \tag{1}$$

where k is the rate constant, t is the reaction time, and $G(\alpha)$ is a function dependent on the reaction mechanism. Many theoretical model functions have been proposed for $G(\alpha)$ [14–17]; typical $G(\alpha)$ functions are shown in Table 1. The mechanism of the dehydration, i.e. the model function for the present dehydration, was determined via the linearity of the plots of various $G(\alpha)$ vs. t, in accordance with Eq. (1). The $G(\alpha)$ for the present dehydration tends to vary with dehydration temperature as shown in Table 2.

At higher temperatures such as 85 and 90°C, the dehydration is described by the phase boundary reactions $R_2(\alpha)$ and $R_3(\alpha)$, and the first order reaction, $F_1(\alpha)$. Of these three functions, $R_3(\alpha)$, which applies to a three-dimensional phase boundary reaction or a contracting volume formula, seems to be a suitable function, because it covers the wider ranges of the dehydration fractions, α.

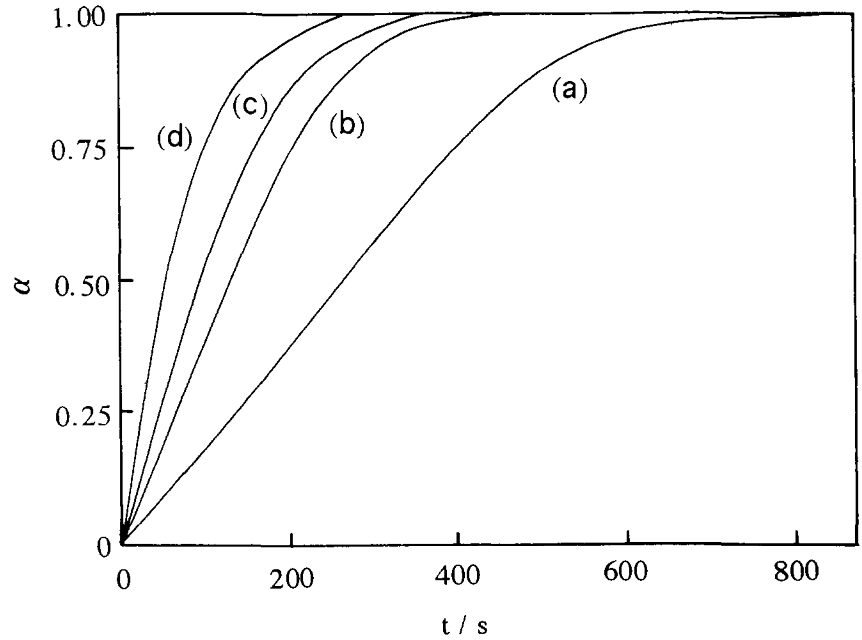

Fig. 1. Typical $\alpha(t)$ curves for the dehydration of $CaCu(CH_3CO_2)_4 \cdot 6H_2O$: (a) 70°C; (b) 80°C; (c) 85°C; and (d) 90°C.

Table 1
Commonly used $G(\alpha)$ for solid-phase reactions

$G(\alpha)$	Symbol	Rate-controlling process
α^2	D_1	One-dimensional diffusion
$\alpha + (1-\alpha)\ln(1-\alpha)$	D_2	Two-dimensional diffusion
$(1-(1-\alpha)^{\frac{1}{3}})^2$	D_3	Three-dimensional diffusion; Jander equation
$1 - 2\alpha/3 - (1-\alpha)^{\frac{2}{3}}$	D_4	Three-dimensional diffusion; Ginstring–Brounshtein equation
$1-(1-\alpha)^{\frac{1}{2}}$	R_2	Two-dimensional phase boundary reaction
$1-(1-\alpha)^{\frac{1}{3}}$	R_3	Three-dimensional phase boundary reaction
$-\ln(1-\alpha)$	F_1	First-order reaction
$[-\ln(1-\alpha)]^{\frac{1}{m}}$	A_m	Avrami–Erofeev equation, $m = 1, 2, 2.5, 3, \ldots$

Table 2
Variation of $G(\alpha)$ for the dehydration of $CaCu(CH_3CO_2)_4 \cdot 6H_2O$

T/°C	$G(\alpha)$	Range of α	C[a]	$\ln k$
90	R_2	0–0.59	1.0000	−5.008
	R_3	0–0.85	0.9999	−5.344
	F_1	0–0.56	0.9986	−4.116
85	R_2	0–0.77	0.9999	−5.517
	R_3	0–0.91	0.9997	−4.698
	F_1	0–0.46	0.9986	−4.697
80	R_2	0–0.39	0.9999	−5.932
	R_3	0–0.39	0.9999	−6.300
	F_1	0–0.37	0.9996	−5.130
	A_2	0.19–0.69	1.0000	−5.220
	$A_{2.5}$	0.19–0.74	0.9998	−5.389
	A_3	0.30–0.84	0.9999	−5.556
	D_2	0.74–0.94	0.9999	−5.215
	D_3	0.80–0.97	0.9999	−5.462
	D_4	0.81–0.97	0.9998	−6.354
70	R_2	0–0.40	0.9996	−6.660
	R_3	0–0.40	0.9995	−7.036
	F_1	0–0.39	0.9987	−5.861
	A_2	0.14–0.69	0.9998	−5.891
	$A_{2.5}$	0.17–0.85	0.9999	−6.055
	A_3	0.22–0.90	0.9999	−6.188
	D_2	0.69–0.94	0.9999	−5.900
	D_3	0.88–0.96	0.9999	−6.166
	D_4	0.75–0.96	0.9998	−7.049

[a] Correlation coefficient.

At temperatures lower than 80°C, the kinetic behavior is extremely complicated. The kinetics of the initial part of the dehydration can be described by the phase boundary reactions, $R_3(\alpha)$, and those of the middle part follow Avrami–Erofeev type reactions, $A_2(\alpha)$, $A_{2.5}(\alpha)$, and $A_3(\alpha)$. The reaction $A_{2.5}(\alpha)$ seems to be the most acceptable of these three mode functions. The kinetics of the final part follow the diffusion-controlled model, $D_2(\alpha)$, $D_3(\alpha)$, or $D_4(\alpha)$. Table 2 shows the rate constants for these functions determined from the slopes of the $G(\alpha)$ vs. t plots at various temperatures. The activation energies, E and pre-exponential factors, A were determined from the Arrhenius plots (Figs. 2 and 3) of the rate constants and are shown in Table 3.

4. Discussion

The present results indicate that the dehydration

$$CaCu(CH_3CO_2)_4 \cdot 6H_2O \rightarrow CaCu(CH_3CO_2)_4 + 6H_2O$$

is an extremely complex process, and that the rate-controlling steps vary with temperature.

It has been shown that the $R_3(\alpha)$ model is characterized by rapid initial nucleation followed by production of a complete reactant–product interface around the preferred crystallographic surfaces, and that the rate depends only on the advance of the reaction interface into the center of sample particle. In this dehydration, many potential nucleus-forming sites may exist on the surface of sample particles which are prepared

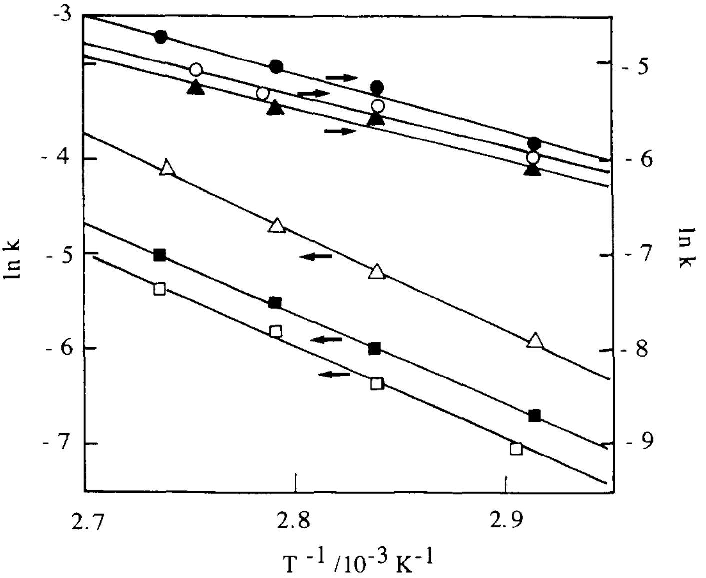

Fig. 2. Arrhenius plots (I): ●, A_2; ○, $A_{2.5}$; ▲, A_3; △, F_1; ■, R_2; and □, R_3.

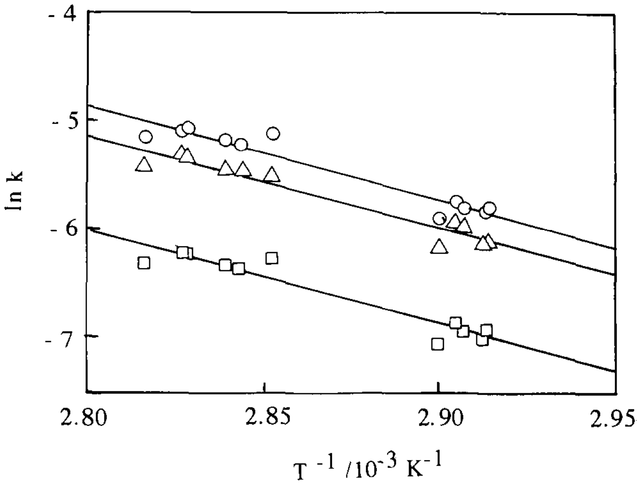

Fig. 3. Arrhenius plots (II): ○, D_2; △, D_3; and □, D_4.

Table 3
Activation energy, *E* and pre-exponential factor, *A*

$G(\alpha)$	E/kJ mol^{-1}	A/s^{-1}
R_2	78.8	1.20×10^9
R_3	81.3	1.98×10^9
F_1	86.4	3.75×10^{10}
A_2	52.5	2.88×10^5
$A_{2.5}$	53.9	3.57×10^5
A_3	45.2	1.72×10^4
D_2	71.3	2.03×10^8
D_3	68.9	6.84×10^7
D_4	71.4	6.88×10^7

by crushing single crystals. Therefore, it seems likely that the reactant–product interface is produced around the surface by rapid growth of these nuclei especially at higher temperatures, and the kinetics are described by the three-dimensional phase boundary model $R_3(\alpha)$.

The Avrami–Erofeev equation

$$[-\ln(1-\alpha)]^{1/n} = kt \qquad (2)$$

is the kinetic expression appropriate to random nucleation and the nuclei growth process, and it has been shown that the parameter *n* depends on the nucleation rate, the geometry of the nuclei, and the growth mechanism, such as diffusion-controlled or phase-boundary-controlled. Hulbert [15] summarized nuclei growth conditions and pointed out the relationship between nuclei growth and the diffusion process of migrating species as follows. When (i) the nucleation rate is assumed to be constant, (ii) the nuclei grow three-dimensionally, and (iii) the growth is controlled by the diffusion of migrating species, the $A_{2.5}(\alpha)$ equation can be derived.

It is most improbable that the dehydration mechanism suddenly changes from $R_3(\alpha)$ to $A_{2.5}(\alpha)$ at a certain value of the dehydration fraction. The transition may be discussed on the basis of appropriate assumptions as follows. The kinetics of the present dehydration seem to depend on the diffusion of the dissociated water molecules. The water molecules dissociated from the "solvent cages" may move through the dislocation network of the reactant and active potential nuclei, particularly in the vicinity of the reaction interface [18]. Thus a reaction zone, where potential nucleus-forming sites are activated, must be developed in front of an advancing interface. The dissociated water molecules may propagate through an amorphous phase of dehydrated products to the surface of sample particle, and then finally leave the surface.

At higher temperatures, the dissociated water molecules may reach the outer surfaces so rapidly that the dehydration seems to follow the $R_3(\alpha)$ model. The diffusion of the dissociated water molecules through the amorphous phase is not negligible at lower temperatures, and the kinetics may apparently be described by a Avrami–Erofeev equation, $A_{2.5}(\alpha)$, derived originally from a diffusion-limited model.

It seems reasonable that the final parts of dehydration are also described by the diffusion model functions, $D_2(\alpha)$, $D_3(\alpha)$, and $D_4(\alpha)$. A decision about which of these three functions is the best fit cannot yet be made. A clue to aid determination of the model function for the present dehydration may be found from kinetic analysis of the dehydration of single crystal samples and from experiments performed under nonisothermal conditions.

References

[1] B.N. Figgs, M. Gerloch, J. Lewis and R.C. Slade, J. Chem. Soc. A: (1968) 2028.
[2] A.K. Gregson and S. Mitra, J. Chem. Phys., 50 (1969) 2021.
[3] J.N. McElearney, D.B. Losee, S. Merchant and R.L. Carlin, J. Chem. Phys., 54 (1971) 4585.
[4] Y. Numasawa, H. Kitaguchi and T. Watanabe, J. Phys. Soc. Jpn., 3 (1975) 1415.
[5] D.E. Billing, B.J. Hathaway and P. Nicholls, J. Chem. Soc. A: (1970) 1877.
[6] F.E. Mabbs and W.R. Smail, J. Chem. Soc. A: (1970) 1716.
[7] D.W. Smith, J. Chem. Soc. A: (1971) 1209.
[8] D.A. Langs and C. Hare, Chem. Commun., (1967) 890.
[9] E.A. Klop, A.J.M. Duisenberg and A.L. Spek, Acta Crystallogr. Sect. C: (1983) 1342.
[10] Y. Masuda, K. Iwata, R. Ito and Y. Ito, J. Phys. Chem., 91 (1987) 6543.
[11] Y. Mausda and K. Nagagata, Thermochim. Acta, 161 (1990) 55.
[12] Y. Masuda and Y. Ito, J. Therm. Anal., 38 (1992) 1793.
[13] Y. Masuda, K. Hirata and Y. Ito, Thermochim. Acta, 203 (1992) 289.
[14] J.H. Sharp, G.W. Brindley and B.N.N. Achar, J. Am. Ceram. Soc., 49 (1966) 379.
[15] S.F. Hulbert, J. Br. Ceram. Soc., 6 (1969) 11.
[16] J. Sestak and G. Berggren, Thermochim. Acta, 3 (1971) 1.
[17] K. Heide, W. Holand, H. Golker, K. Seyfrarth, B. Muller and R. Sauer, Thermochim. Acta, 13 (1975) 365.
[18] R.A.W. Hill, Trans. Faraday Soc., 54 (1958) 685.